THE JOURNAL OF PHYSICAL CHEMISTRY C
A JOURNAL OF THE AMERICAN CHEMICAL SOCIETY

pubs.acs.org/JPCC

Article

Single-Molecule SERS Hotspot Dynamics in Both Dry and Aqueous Environments

Published as part of The Journal of Physical Chemistry virtual special issue "Nanophotonics for Chemical Imaging and Spectroscopy".

Nathan C. Lindquist,* Ariadne Tückmantel Bido, and Alexandre G. Brolo*

Cite This: *J. Phys. Chem. C* 2022, 126, 7117–7126

Read Online

ACCESS | Metrics & More | Article Recommendations | Supporting Information

ABSTRACT: Fluctuations in Surface Enhanced Raman Spectroscopy (SERS) signals are a hallmark of few-to-single molecule events. Recent experiments have shown these SERS intensity fluctuations (SIFs) to occur over an extremely wide range of time scales, from seconds to microseconds. While many mechanisms have been proposed, such as molecular diffusion or transient plasmonic hotspot generation, the underlying source of these fluctuations is likely to be a complex interplay of different effects. For example, SERS experiments done with fully coated, but dry, nanoparticles would have less movement of the probe molecule but may still have transient hotspot generation due to the mobility of metallic atoms. Alternatively, experiments done with low concentrations of a molecular probe in liquid might tend to see fluctuations caused by freely diffusing molecules that visit and become trapped within a static hotspot. In this paper we compare high-speed SIF activity in both dry and wet nanoparticle environments. By carefully analyzing the overall SERS signal fluctuations, such as the timing statistics, we propose a simple model that accounts for the contributions from the various mechanisms discussed above. These results provide a deeper physical understanding of the SERS effect and may promote further research into single-molecule SERS, its experimental optimization, and potential applications.

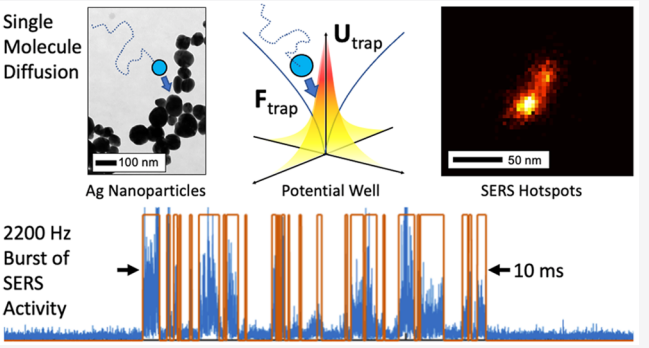

INTRODUCTION

Understanding the interaction of light and matter on the nanoscale is an active area of fundamental research with a wide range of important applications from developing fast and efficient biosensors to creating novel optoelectronic devices.[1] To pursue these goals, it is paramount to explore light-matter interaction down to the single photon, single atom, single molecule, and single nanoparticle regimes. Surface enhanced Raman spectroscopy (SERS) is a well-known and highly studied effect that represents well the challenges and opportunities inherent to nanophotonics and nanotechnology.[2−4] The SERS effect is the large enhancement in Raman scattering seen from molecules that are in regions of concentrated electric fields generated in illuminated metallic nanostructures.[5] These highly localized electric fields or "hotspots" are created by the excitation of localized surface plasmon resonances. These localized SERS hotspots are much smaller than the wavelength of the illuminating light, perhaps approaching atomic dimensions.[6,7] The resonance behavior of these hotspots depends highly on the local nanoenvironment. With such nanofocused light, single-molecule behavior is readily observed,[8,9] with one of the hallmarks being fluctuations in the overall SERS intensity and spectral features.[10−12] Recent experiments done with extremely high-speed imaging revealed that the fluctuations occur over a wide range of time-scales, from tens of seconds down to single microseconds.[13,14] Super-resolution imaging and experiments with multiple laser wavelengths and polarization states[15] showed that SIFs occur on the subnanoparticle level in hyper-localized (<10 nm) regions of the larger nanoparticle (~100 nm). These experiments suggest that intensity fluctuations, which occur in different combinations of probe molecule and nanoparticle shape, size, and material,[16] are a universal and fundamental characteristic of the SERS effect that becomes more and more relevant with high-speed or single-molecule experiments. While many mechanisms have been proposed for such SIF behavior, early reports of single-

Received: January 14, 2022
Revised: March 11, 2022
Published: April 13, 2022

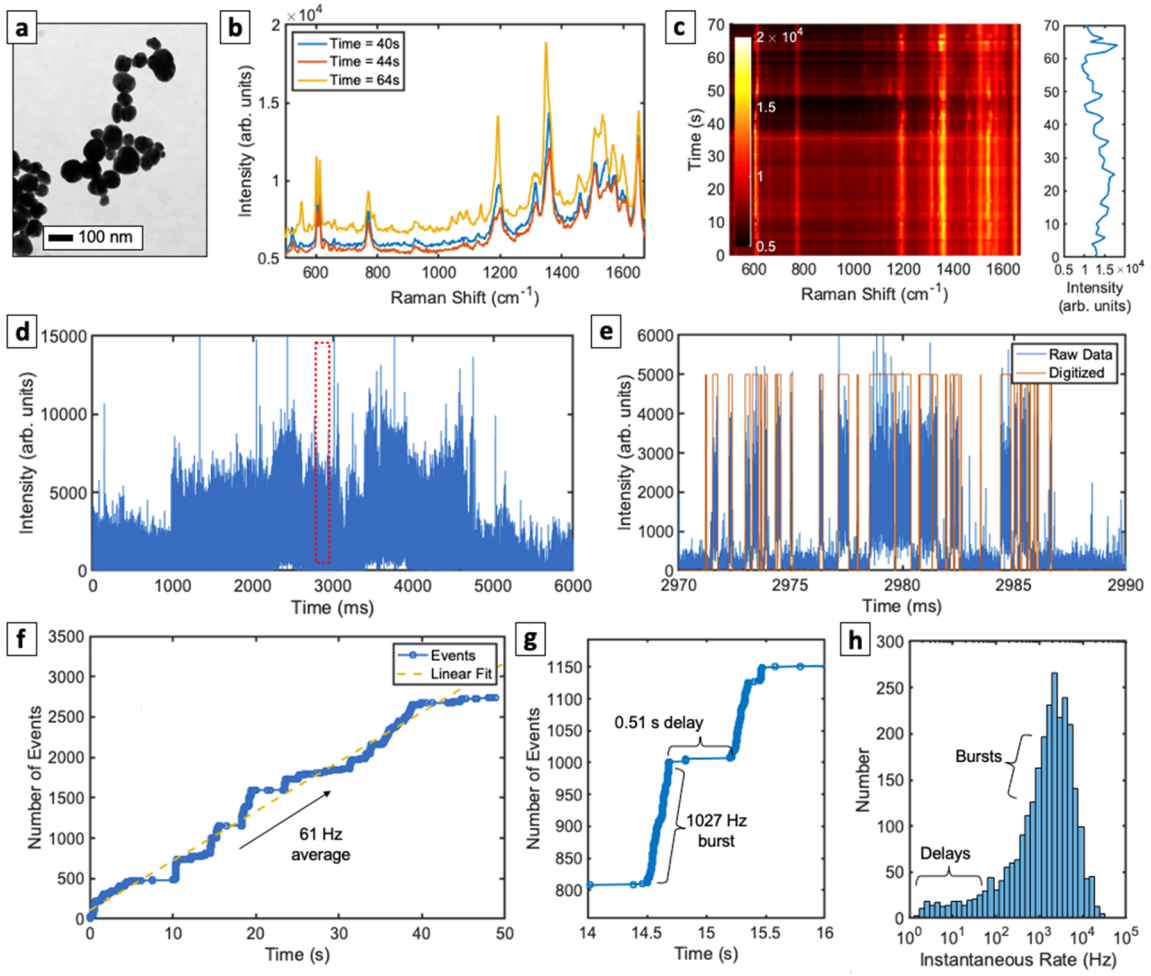

Figure 1. High-speed SERS with dry nanoparticle clusters. (a) TEM image of silver nanoparticle clusters dried on a glass coverslip. (b) SERS spectrum of the nanoparticles coated and dried with a 50 nM solution of R6G, from three different times several seconds apart. (c) A time-series spectrum showing intensity fluctuations over the course of 70 s. Also shown in the side insert is the fluctuating intensity of the peak near 1360 cm^{-1}. (d) Recording on a fast point PMT detector shows that these fluctuations occur on multiple time scales. The red boxed area is zoomed in and (e) shows a sequence of very fast bursts on the 10s of μs time scale. The fluctuations can be digitized and counted. (f) Plotting the event count versus time of another sample shows an average rate of 61.4 Hz for this particular sample. (g) Zooming in shows that the signal is composed of rapid bursts followed by longer delays. (h) Histogram of the instantaneous event rate showing the regimes of fast bursts and slower delays.

molecule SERS relied on very low concentrations of molecules, such that only one molecule, on average, would be in a plasmonic hotspot at any given time.[17] This is similar to single-molecule fluorescence experiments.[18] However, experiments with large numbers of surface molecules also show significant SIF behavior.[19] Just as the underlying mechanism to SERS itself includes multiple effects such as electromagnetic[20] and chemical enhancement,[21] the mechanism of high-speed SERS fluctuations is likely to be a complex interplay of multiple contributions. For example, SERS experiments done with fully coated, but dry, nanoparticles would perhaps have less movement of the probe molecule but may still have transient hotspot generation due to the mobility of metallic atoms. Alternatively, experiments done with low concentrations of a molecular probe in liquid might tend to see fluctuations caused by freely floating molecules that visit and become trapped within a static hotspot. These effects may occur over different time scales, with different optical resonance conditions, and be enhanced or suppressed with different experimental conditions such as sample temperature. In this paper, we explore various experimental conditions for single-molecule SERS that all show high-speed SERS intensity fluctuations (SIFs): (1) rhodamine 6G molecules (R6G) dried onto silver nanoparticle clusters and (2) R6G molecules in solution over wet silver nanoparticle clusters. The probe molecule and the SERS substrate are identical, yet the local environments are unique. By carefully analyzing the overall SIFs, such as the timing statistics, we propose a simple model that accounts for the contributions from the various mechanisms discussed above.

METHODS

Silver Nanoparticles (AgNPs) were prepared according to Leopold and Lendl.[22] Briefly, in a beaker containing 89 mL of a 3.33 mM sodium hydroxide solution, 1 mL of a 150 mM hydroxylamine hydrochloride solution was added. Then, under vigorous stirring (1000 r/min), 10 mL of a 10 mM silver nitrate solution were added dropwise. The mixture was left stirring for 15 min, resulting in a brown-greyish colored solution. The synthesized AgNPs were then stored at 4 °C. The TEM images of the AgNPs resulted in mostly spherical particles with estimated average size of 43 ± 17 nm.

https://doi.org/10.1021/acs.jpcc.2c00319
J. Phys. Chem. C 2022, 126, 7117−7126

Microscope round glass coverslips were cleaned with piranha solution, consisting of three parts of sulfuric acid to one part 30% hydrogen peroxide to remove any organic matter that may be present. This was followed by washing abundantly with ultrapure water and subsequent drying in N_2 flow. For the "dry" system, 10 μL of the AgNPs were dropped on top of a clean glass coverslip and left to dry. Next, 10 μL of a Rhodamine 6G solution in water with a determined concentration, ranging from 10 to 100 nM, were dropped on top of the previously dried AgNPs and left to dry. These slides were then measured on the confocal microscope. For the "wet" system, 10 μL of the AgNPs were dropped on top of a clean glass coverslip and left to dry. Next, the coverslip was assembled in a custom-made metal holder, followed by the addition of a Rhodamine 6G solution in water with a determined concentration, ranging from 10 to 100 nM, enough to cover the slide. Finally, we also imaged AgNPs with covalently bonded molecules. A 5 mL sample of AgNPs was incubated at room temperature overnight with 250 μL of a 10 mM solution of 5,5′-dithiobis(2-nitrobenzoic acid) (DTNB) in ethanol. The mixture was then centrifuged at 15 000 rpm for 20 min, the supernatant is discarded, and the particles were resuspended in 5 mL of deionized water. A 10 μL aliquot of this solution was then dropped and dried on a clean glass coverslip. All of these sample slides were then measured on the confocal microscope, focusing on the AgNPs that were deposited on the glass.

We then considered two experimental conditions, and both showed high-speed SIF behavior: (1) a set of "dry" samples that consisted of Ag nanoparticles clusters fully coated with R6G molecules and dried on a glass coverslip; (2) a set of "wet" samples that consisted of bare Ag nanoparticle clusters dried on a glass coverslip that were then measured in the aqueous media at various concentrations of R6G. The samples were loaded into a commercial microscope (Zeiss- LSM 880, AxioObserver) that had both high-speed photomultiplier tubes (PMTs) and a high-speed 32-channel Airyscan detector typically used for enhanced resolution in a laser-scanning imaging arrangement,[23] but that can also be used for high-speed imaging, up to 804,000 frames per second, though with the field of view limited to 32 pixels.[14] Point scans with a single PMT detector were also digitized at a rate of 804,000 samples per second. The dry coverslip samples were imaged with an oil-immersion objective (63×, NA = 1.40). The wet coverslip samples were imaged with an LD EC Epiplan-Neofluar (50×, NA = 0.55). Both were illuminated with a green laser (wavelength of 543 nm) and total laser power of 5% or 10%, as set by the commercial instrument software.

Using a set of optical filters, the entire Stokes shifted region, from 134.7 to 4810.8 cm^{-1}, was collected at high speeds with the single-photon-sensitive PMT detectors. The acquisition time was 1.24 μs, representing an acquisition rate of 0.806 MHz, fast enough to capture SIF events that occur on the order of 10s of μs. These SIF trajectories were captured over the course of 1 min. We also used a commercial Raman microscope (Renishaw inVia Raman Microscope with a Centrus detector) to capture a full SERS spectrum on similar samples. While the slower Raman microscope and spectrometer also showed SIF behavior, the high-speed acquisitions reveal that these are actually composed of multiple faster events. The coverslips were measured with a 50× (NA = 0.75) objective for 100 total acquisitions of 1 ms each (total exposure time 1 s) with a 532 nm laser at 0.5 mW to 1 mW power. The spectrometer used a 1200 l/mm grating to capture a Raman shift range from 420 to 1620 cm^{-1}.

RESULTS AND DISCUSSION

Figure 1 shows a representative set of data taken from a "dry" nanoparticle cluster coated with R6G molecules. A transmission electron microscope (TEM) image of the nanoparticle clusters is shown in Figure 1a. The nanoparticles themselves range in size from ∼30 nm to ∼100 nm and when dried onto the coverslip will naturally form small clusters. These clusters provide ideal arrangements of nanoparticle dimers, trimers, and tetramers that are known to generate intense localized SERS hotspots.[16] A representative spectrum from the Raman microscope is shown in Figure 1b. Two other spectra taken at two different times are also shown, revealing SIF behavior. While there is some background offset, e.g. due to fluorescence of the R6G molecules, the SERS peaks themselves are pronounced and show significant fluctuation activity. A waterfall plot of time series of SERS spectra, each with an acquisition and exposure time of 1 s and taken sequentially over ∼1 min, is shown in Figure 1c, again revealing the SERS fluctuations in time. A plot of the intensity of the peak near 1360 cm^{-1} is shown in the side panel. While SIF events are observed in the slower Raman spectrometer setup, high-speed measurements on a similar sample reveal that the fluctuations are actually composed of both millisecond features (Figure 1d) and microsecond features (Figure 1e). While we cannot entirely neglect the contributions from fluorescence or other background signals in the fast point PMT scans, the prominent SERS peaks in the spectrometer data seem to indicate that the majority of our fluctuating signal is due to SERS. The SIF events are distinct enough that they can be digitized, in an ON/OFF manner, using a "cumulative sum" anomaly detection algorithm as developed in previous reports.[14] The digitized signal is shown over the raw SERS intensity data in Figure 1e. These digitized events can then be further processed to extract, for example, the statistics and time-series behavior of the SIF trajectories. Figure 1f shows the number of SIF events versus time. Over a total acquisition time of 50 s, the dry R6G sample generated SIF events at a rate of roughly 61 Hz. However, upon closer inspection, these SIF events are seen to be very nonuniform in time. Figure 1g zooms in on a region of the SIF trajectory that shows a very fast 1027 Hz "burst" of SIF activity followed by a long 0.51 s "delay" where the SERS signal is dark. Plotting a histogram (Figure 1h) of the instantaneous rate of the SIF events, defined as the inverse of the time delay from one SIF event to the next, shows these regions of extremely high-speed bursts of activity, occurring from 1 kHz to 10 kHz, and the regions of much slower delays from 1 Hz to 10 Hz. In this case, since the nanoparticles are fully coated with the probe molecules, the fluctuations are likely to arise more from the transient nature of the local hotspots rather than the lack of molecules. Recent results with a nanoparticle-on-mirror (NPoM) configuration[7] or a single rough nanoparticle[14] suggest that the fluctuations in these cases are driven by a transient increase in the local hotspot strength due to atomic reconstruction. In other words, a single hotspot finds a molecule instead of the molecule finding the hotspot. While a scanning hotspot with atomic resolution[24] is the driving concept behind tip-enhanced Raman spectroscopy (TERS), this is a new concept in SERS and suggests a dynamic, rather than a static, distribution of hotspots over the surface.

https://doi.org/10.1021/acs.jpcc.2c00319
J. Phys. Chem. C 2022, 126, 7117−7126

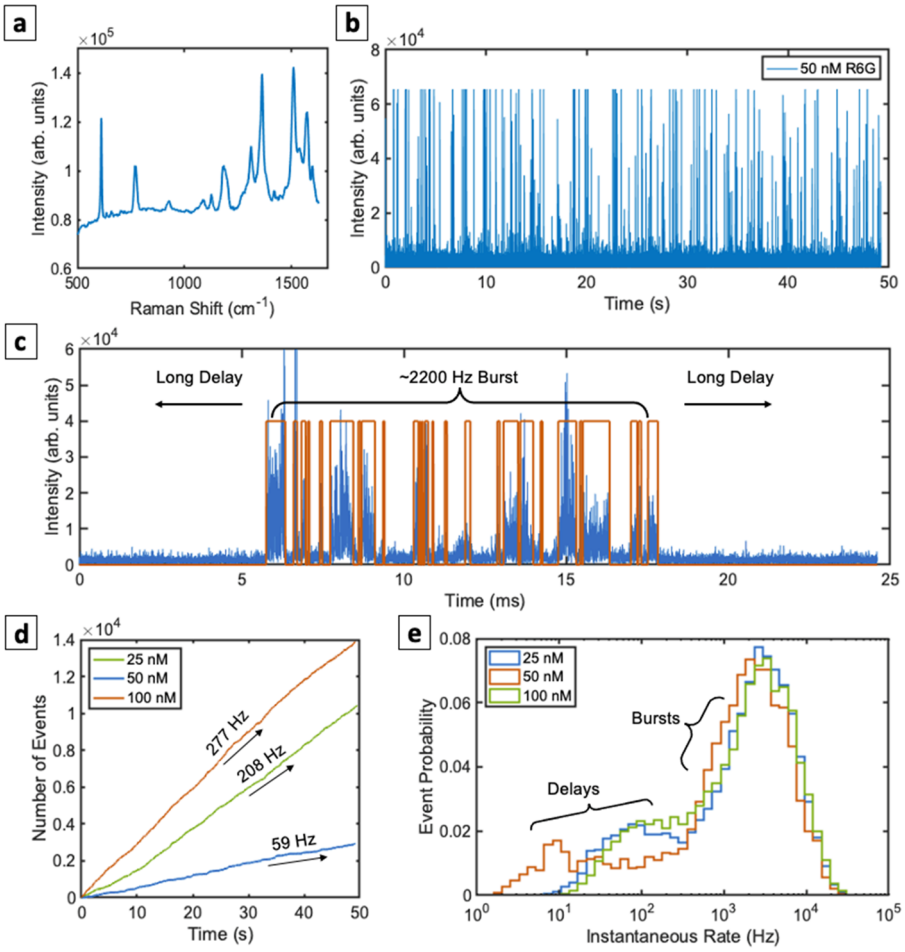

Figure 2. High-speed SERS with wet nanoparticle clusters (immersed in aqueous solutions of R6G). (a) Sample SERS spectrum of a nanoparticle sample immersed in a 50 nM solution. (b) SERS trajectory for a silver nanoparticle cluster sample immersed in a 50 nM R6G dye solution. As before, this sample again shows strong intensity fluctuations. (c) The intensity fluctuations tend to come in bursts at very high speeds. (d) Unlike a dry sample, these wet samples allow experimentation with the molecule concentration. A solution of 100 nM dye fluctuates at a faster average rate. However, the rate is not exactly twice that of the 50 nM solution because this region likely had a different number of hotspots within the focal volume of the laser. Similarly, a 25 nM solution fluctuates nearly as fast as the 10 nM solution. (e) The signals are composed of fast bursts and longer delays. Interestingly, the fast ~5000 Hz of the three concentrations are similar whereas the delays are ~10× slower in the 50 nM solution. This suggests that the 25 nM and 100 nM particles had more events due primarily to more active hotspots and not the number of available molecules.

In contrast to the "dry" nanoparticle samples, we also explored "wet" nanoparticle samples. In this case, it is trivial to alter the availability of probe molecules by altering the concentration of the solution. The silver nanoparticle clusters were bare and dried to the glass coverslip before incubation. Figure 2a shows a sample SERS spectrum from a wet nanoparticle cluster, i.e., immersed in 50 nM R6G aqueous solution. As before, while there is a fluorescence background, the SERS peaks are still quite prominent. An ~50 s long high-speed PMT trajectory is shown in Figure 2b, showing strong fluctuations. While the signal in this case may be a combination of both SERS and fluorescence, and, indeed, the "SIF" acronym could be understood to include all "surface-enhanced intensity fluctuations," Figure 2c shows that the signal behavior is again characterized by brief periods of high-speed fluctuations followed by long delays. This seems to indicate that the time dynamics of the SIFs may be driven by the transient hotspot generation since a dry sample shows similar behavior. In fact, the concentration of the solution, while having an effect, does not correlate exactly to the amount of SIF events. Figure 2d shows SIF event counts for three different nanoparticle clusters incubated with three different concentrations. The nanoparticle cluster incubated with a 100 nM solution generates more SIF events overall at a higher rate than the nanoparticle cluster incubated with a 50 nM solution. However, a sample incubated with a 25 nM solution shows nearly four times the SIF activity than the 50 nM sample. Since each sample was illuminated with the same focused laser spot, this indicates that the number of hotspots was greater in the 25 nM sample than in the 50 nM sample. This is seen also in Figure 2e, where histograms of the instantaneous rates are plotted for the three concentrations. The sample incubated with 50 nM solution had more and longer periods of inactivity, whereas the 25 nM and the 10 nM samples were similar. These observations confirm that the high-speed experiments probe local hotspot behaviors that are not controlled in random metallic clusters.

Imaging the nanoparticle clusters, in addition to the timing statistics above, further emphasizes that the SIF behavior is a combination of the availability of the molecules and the availability of a hotspot. While point PMT scans could show an unusually fast SIF rate that may hint at more than one hotspot,

https://doi.org/10.1021/acs.jpcc.2c00319
J. Phys. Chem. C 2022, 126, 7117−7126

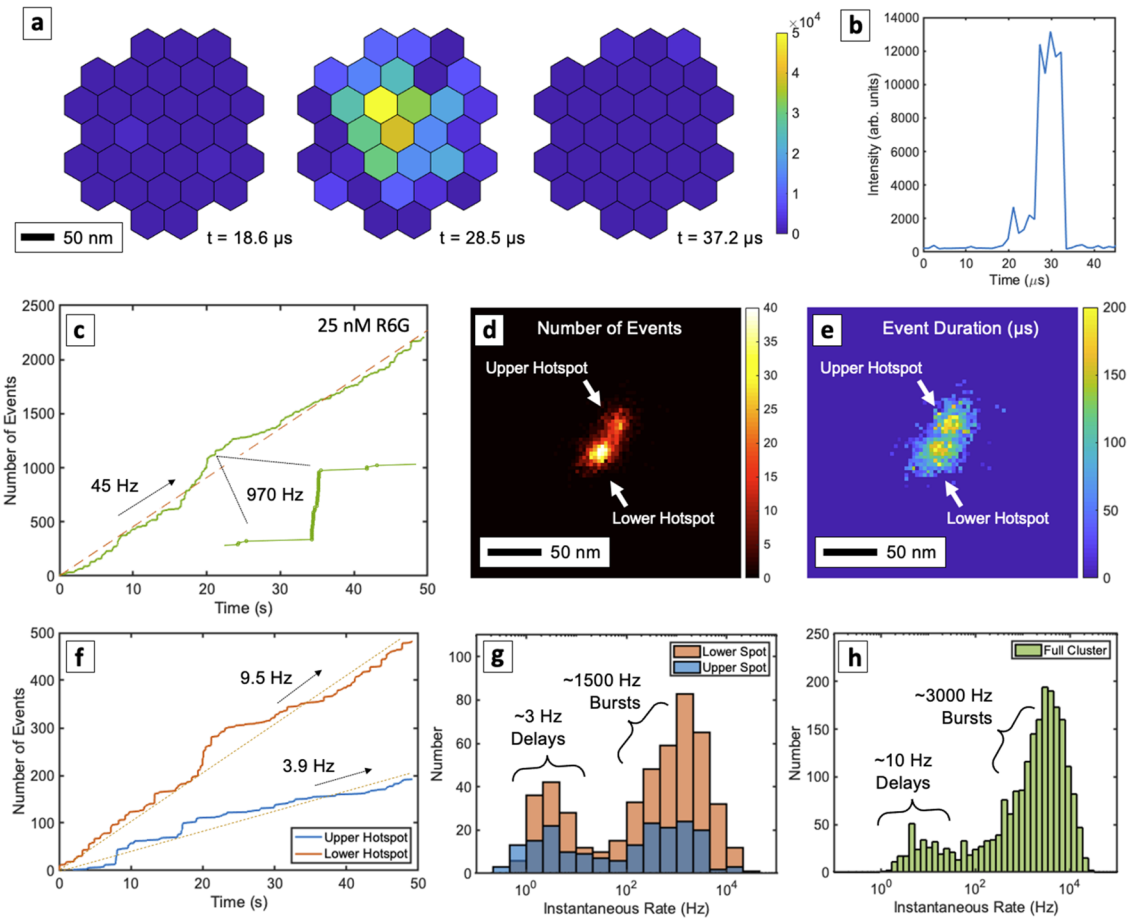

Figure 3. High-speed imaging of the localized hotspots in a wet nanoparticle cluster (immersed in R6G aqueous solutions). (a) Raw data on the high-speed Airyscan detector showing a fast ∼10 μs event. (b) Trajectory of the mean value of the 32 pixels. (c) Plotting event count in time for the nanoparticle cluster with an average rate of 45 Hz and brief bursts as before. (d) Fitting the data from the 32 pixel Airyscan detector to a 2D Gaussian function (localization procedure) reveals the events occurring at two distinct hotspot locations. (e) The hotspots appear similar in their average event duration but (f) their local fluctuation rates are different. The lower hotspot fluctuates on average faster than the upper hotspot, resulting in more events overall. (g) Histograms of the instantaneous event rate for the two hotspots, again showing two distinct time scales of longer delays with short bursts of activity. (h) Histogram of the entire particle (i.e., without being spatially resolved) shows a skewed time scale due to the presence of more than one unique hotspot.

in general it is difficult if not impossible to count hotspots without imaging capability. Figure 3a shows three frames from the high-speed Airyscan detector. Briefly, the point-spread function of the microscope is imaged, i.e. as a diffraction limited spot, onto an array of 32 fiber-coupled PMT detectors. With high-speed digitization of 804,000 frames per second, a high-speed "movie" of the nanoparticle cluster can be recorded. The movie is then processed by fitting a 2D Gaussian function to each frame, localizing the SERS emission centroid and effectively "imaging" the particle with sub-wavelength resolution.[14,25−27] It is important to emphasize here that this is not a perfect one-to-one optical image, since the emitted light couples to the localized surface plasmon resonance (LSPR) of the nanoparticle system.[28] Figure 3b shows the average intensity of all the detectors in time, revealing a single SIF event that lasts only ∼10 μs. As before, these SIF events are characterized by very high-speed bursts on the ∼kHz scale with longer periods of inactivity. The particular sample shown here, immersed in 25 nM R6G solution, had an average SIF event rate of 45 Hz with occasional high-speed bursts, as shown in Figure 3c. However, this behavior was not uniform over the sample. By analyzing the super-resolution image in Figure 3d, it is clear that this nanoparticle cluster was composed of two distinct regions, labeled in Figure 3d as the "upper hotspot" and the "lower hotspot", that are separated spatially by only ∼20 nm. While both hotspots were illuminated by the much larger laser spot, the "lower hotspot" generated more events than the "upper hotspot" (Figure 3d). This shows hotspot-to-hotspot variability, even within deeply subwavelength regions, for the same overall illumination conditions. However, a time analysis, indicated in Figure 3e, showed that both hotspots had similar event durations, in the 10s to 100s of μs. The lower hotspot simply generated more events, perhaps due to a more efficient hotspot, i.e., one that generated more signals above the noise threshold, or perhaps due to that particular hotspot being composed of more than one distinct region that were not spatially resolvable, even on the ∼10 nm scales shown here. Figure 3f shows that, by counting the number of SIF events in time within a circular region defining each hotspot, the lower hotspot generated SIF events at an average rate of about 9.5 Hz whereas the upper hotspot generated events at 3.9 Hz. As before, these occurred over periods of extremely high-speed 1−10 kHz bursts with much slower periods of inactivity. In this regard, the upper and lower hotspots were similar, as shown in the instantaneous rate histograms plotted in Figure 3g, with two very distinct time

https://doi.org/10.1021/acs.jpcc.2c00319
J. Phys. Chem. C 2022, 126, 7117−7126

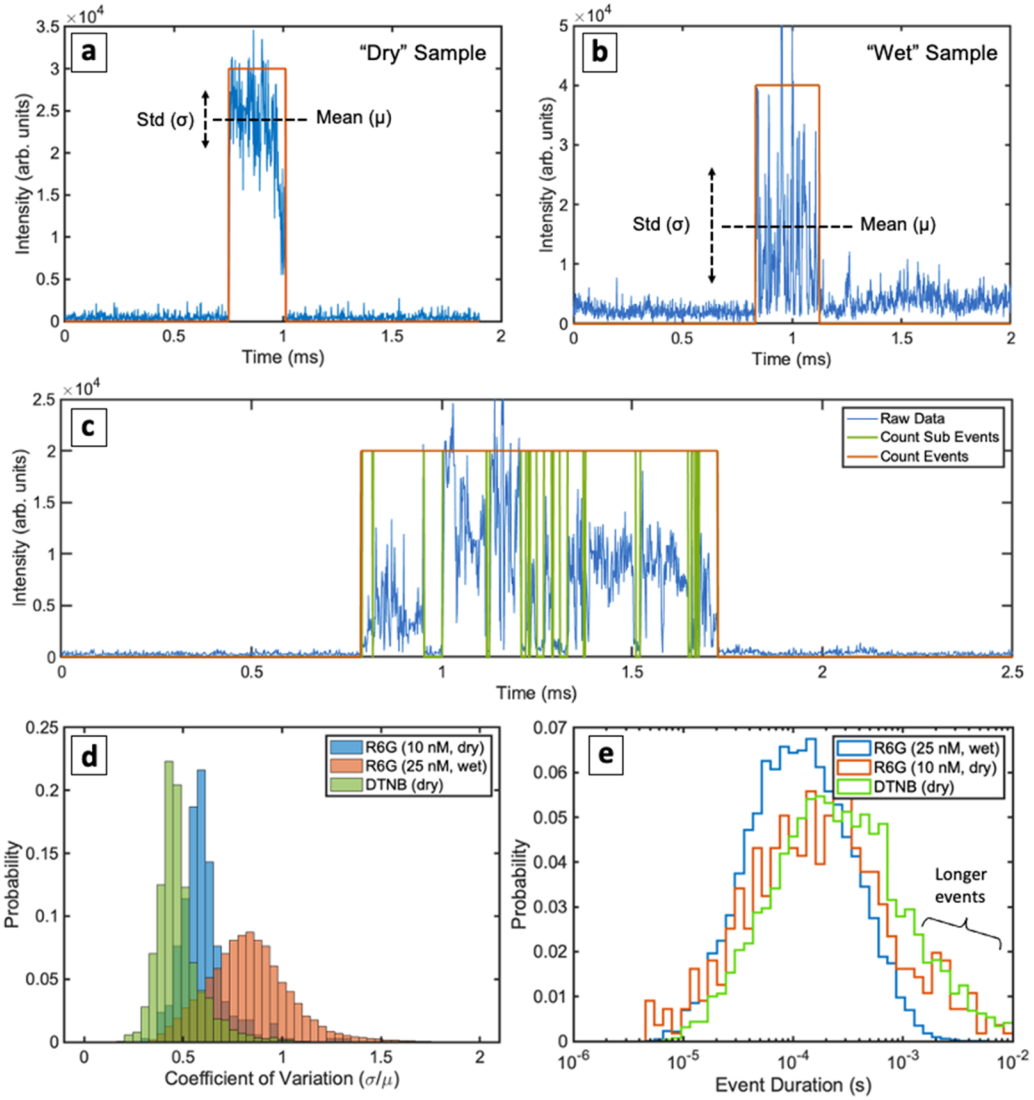

Figure 4. Comparing "wet" versus "dry" samples. (a) A single event on a "dry" nanoparticle cluster sample with dried 10 nM R6G. The event is step-like with a clear ON and OFF. (b) A single event with a "wet" nanoparticle cluster sample with 25 nM R6G. The pulse is much noisier and fluctuates during the event. (c) Another way to classify event characteristics is by adjusting the digitization algorithm sensitivity to quick changes. These could be classified as "sub events" as shown in the green trace. (d) Histogram of the coefficient of variation (CoV) for the wet and dry samples. The wet sample has more variation and a wider distribution. Another dry sample, this time with covalently bonded DTNB, shows an even tighter CoV distribution. (e) In addition to the CoV it is also possible to quantify the event duration. On average the "dry" samples had more long-lasting events.

scales of delays and bursts. Extracting any time statistics from a single nanoparticle or cluster therefore needs to take into account the presence of perhaps more than one unique hotspot. The measurements in Figures 1 and 2 were taken with a single point PMT detector and not the imaging detector used in Figure 3. We therefore did not know how many hotspots were under the laser in those experiments, and it is likely that there were more than one. This is a key motivating factor for the use of imaging experiments. Indeed, Figure 3h shows that by counting all the events, without spatially separating them into distinct hotspot regions, a skewed SIF rate histogram is produced, where both the bursts and the delays appear to be faster than if the hotspots are analyzed separately and on subdiffraction-limited spatial scales. Another example of this rate effect for a different nanoparticle cluster is shown in Supporting Information (SI) Figure S1. Other local effects are also seen in SI Figure S1, such as a hotspot that is "on" for longer times than another hotspot only a few 10s of nm away.

These experiments done with both "wet" and "dry" nanoparticle clusters all showed some basic similarities. Both environments had similar timing behavior of bursts and delays, and both environments indicated that the SIF event generation must be a combination of both the availability of a probe molecule and the availability of a hotspot. While this is clearly central to the entire interpretation of SERS and has been since it was first discovered some decades ago, these results stress the fact that both of these mechanisms are incredibly transient, fluctuate with high speeds, and are very nonuniform even on ∼10 nm spatial scales. However, there were some important differences observed with the wet (substrate immersed in aqueous solutions, as discussed above) versus the dry samples. Figure 4a shows a typical SIF event for a "dry" sample. The event is very digital, with clear ON and OFF states. The SIF

https://doi.org/10.1021/acs.jpcc.2c00319
J. Phys. Chem. C 2022, 126, 7117−7126

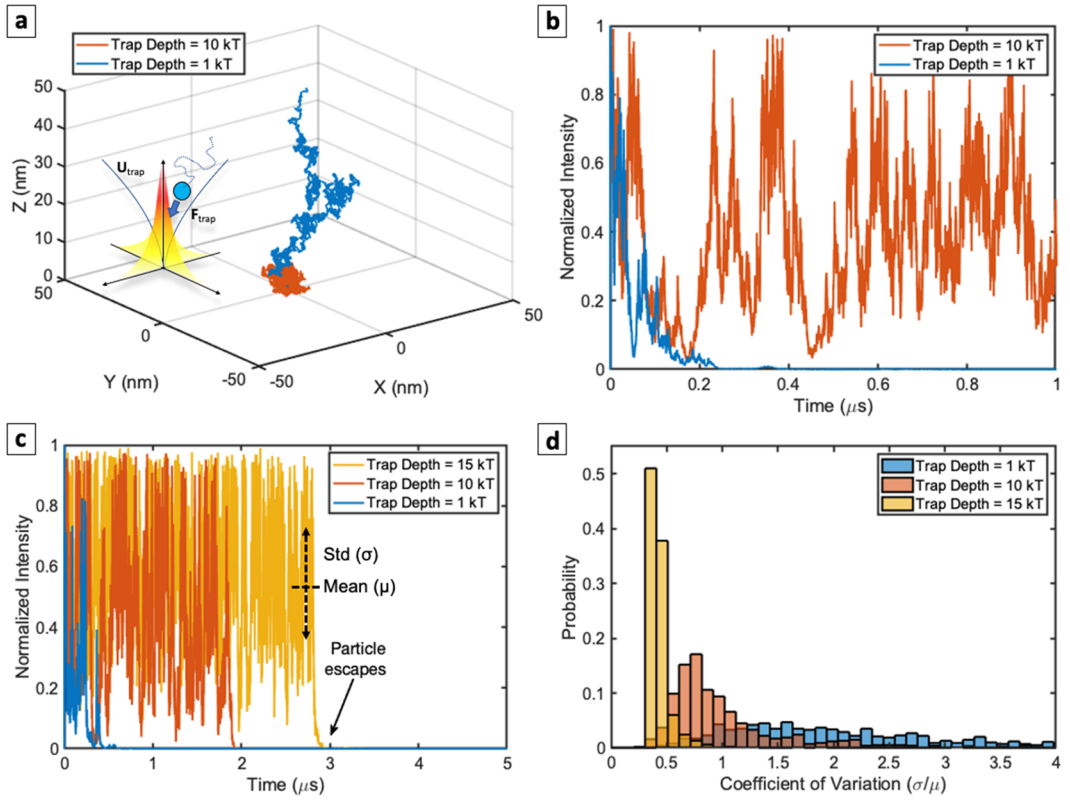

Figure 5. Computer simulations of fluctuation dynamics. (a) Spatial trajectories of a Brownian particle (single molecule) in a potential well with depths equal to the thermal energy kT and 10× the thermal energy. (inset) The potential well is modeled as an exponentially decaying "hotspot" centered at the origin with a typical decay length of 10 nm in the $\pm x$, $\pm y$, and $+z$ directions. The particle begins at the trap center and is allowed to diffuse under Brownian motion and the simulated trap forces. (b) Mapping the position of the molecule to a simulated intensity of the particle/hotspot system shows strong signal fluctuations. Only the first μs is shown here, but (c) tracking for longer times shows that the particle may eventually leave the trap. The deeper traps show longer trap times as well as a less noisy signal. (d) Coefficient of variation for 1000 simulations at each trap depth. Each simulation stops when the particle leaves the trap. The deeper traps show less variation and a more stable signal.

event average intensity is well above the background, and the signal does not fluctuate appreciably while it is ON. In other words, the mean intensity (μ) of the SIF event is large compared to the standard deviation (σ) of the SIF event. The ratio σ/μ is called the "coefficient of variation" and is a standard measurement of the relative noise level of a signal.[29] Figure 4b shows a typical "wet" SIF event which clearly presents a larger coefficient of variation (CoV). In other words, the signal tends to fluctuate more during a single SIF event for a wet sample in aqueous solution versus a dry sample. It is possible that the SIF events with large CoVs are actually multiple faster single events. This can be tested by adjusting the sensitivity to quick changes of the digitization algorithm, shown in Figure 4c. This captures many more events that we could classify as "sub-events" of a longer single event. However, even after adjusting the sensitivity threshold to capture as many events as possible, the CoV or noisiness of a single captured event stays relatively constant and there is still a significant separation between a "wet" and a "dry" sample (see SI Figure S2). In other words, the differences seen in the CoV are not due to the algorithm and its chosen sensitivity thresholds, but rather due to the nature of the signal itself. This can be seen further by plotting a histogram of the CoV for all SIF events observed for a particular experiment, shown in Figure 4d. The wet sample had a broad CoV distribution whereas the dry sample had a narrower distribution. Another set of dry nanoparticles, this time coated with covalently bonded 5,5′-dithio-bis(2-nitrobenzoic acid) (DTNB) molecules, showed an even narrower distribution. Representative SIF trajectory data for a dried DTNB sample are shown in SI Figure S3. Overall, the average CoV for 8 different "wet" nanoparticle samples incubated with R6G was 0.82 whereas it was 0.65 for 13 different "dry" nanoparticle clusters coated with R6G. The 5 different samples with covalently bonded DTNB molecules had an average CoV of 0.55. These results indicate that loosely bound molecules, e.g. those freely floating in liquid, will generate noisier SIF events than more tightly bound molecules, e.g. the dried and adsorbed R6G molecules or the covalently bonded DTNB molecules. Finally, the dried samples fully coated with molecules also tended to generate longer-lived SIF events, shown in Figure 4e. The average SIF event duration for the 8 different wet samples was 213 μs whereas the average SIF event duration for the 13 different dry samples was 1224 μs. This is perhaps due to a surface-stabilizing effect wherein the transient hotspots generated by movement of the silver atoms also become more stable. The several samples coated with DTNB also had a longer average SIF event duration of 768 μs, a sample histogram of which is also shown in Figure 4e.

The experimental results presented in Figures 2 − 4 clearly indicate different behaviors for single molecules on SERS surfaces under "dry" and "wet" conditions. For dry conditions, the results imply that while the hotspots are activated, the molecules trapped in that region experience relative stability. On the other hand, in wet conditions, the molecule can diffuse in solution, providing another channel for time-dependent

https://doi.org/10.1021/acs.jpcc.2c00319
J. Phys. Chem. C 2022, 126, 7117−7126

fluctuations.[30] This can be imagined as single molecules experiencing more Brownian influence when the surface is immersed in a liquid than for the dry sample. Therefore, to further consider the difference in the CoV between "wet" and "dry" environments, we developed a simple numerical model of a small particle (single molecule) trapped in a potential well. The particle undergoes Brownian motion and experiences forces due to the trapping potential, shown schematically in Figure 5a (inset). Here, the trapping potential is explicitly considered to be the optical or plasmonic forces $F(x)$ on the particle due to the SERS hotspot, but it could also represent other general surface or binding forces that the particle (single molecule) might experience. We modeled the position $x(t)$ of a particle of mass m with the Langevin equation

$$m\ddot{x}(t) = -\gamma\dot{x}(t) + F(x) + \sqrt{2k_BT\gamma}\,W(t) \quad (1)$$

where γ is the friction coefficient, $\sqrt{2k_BT\gamma}\,W(t)$ is a stochastic Brownian motion force acting on the particle, k_B is Boltzmann's constant, and T is the absolute temperature. We set temperature T = 300 K, mass $m = 10^{-24}$ kg (order of magnitude mass of an R6G molecule), and the friction coefficient $\gamma = \frac{1}{D_s} = 1.9 \times 10^{-11}$ N s/m, using the Stokes drag coefficient $D_s = 6\pi\eta a$, where a = 1 nm is the radius of the particle and the dynamic viscosity of water is $\eta = 10^{-3}$ N s/m^2. For numerical modeling, a finite-difference approach is taken.[31] In particular, we solve for

$$x(t + \Delta t) = x(t) + \dot{x}(t)\Delta t \quad (2)$$

where Δt is the simulation time step. The stochastic function $W(t)$ then becomes a series of numbers $W(t) = \frac{w(t)}{\sqrt{\Delta t}}$, where $w(t)$ is a series of Gaussian random numbers with a mean of zero and a variance of one.[31] Since in our simulations the particle's momentum relaxation time $\frac{m}{\gamma}$ is on the order of 10^{-14} s, we choose a time step $\Delta t = 10^{-10}$ s to safely model Brownian motion in the diffusive regime while also being able to capture the high-speed dynamics of the particle. This means the inertial term m can be dropped from eq 1. If the simulation step size is too large, the optical trap dynamics will not be captured. Solving for the velocity $\dot{x}(t)$ and inserting into eq 2, the finite difference equation for $x(t + \Delta t)$ becomes

$$x(t + \Delta t) = x(t) + \frac{\Delta t}{\gamma}F(x) + \sqrt{2\frac{k_BT}{\gamma}\Delta t}\,w(t) \quad (3)$$

We note that the quantity $\frac{k_BT}{\gamma}$ can be replaced with the particle's diffusion coefficient D through the Einstein relation $\gamma D = k_BT$. The force $F(x)$ was modeled as that produced from an exponentially decaying "hotspot" centered at the origin. If the potential well U represented by the hotspot varies as $U(x) = -U_0\, e^{-|x|/\delta}$, where δ = 10 nm is the size of the hotspot and U_0 is the depth, the restoring (gradient) force also varies exponentially. For simulations with a three-dimensional potential well the coordinates x, y, and z each update independently according to eq 3. However, while the particle moves freely in x and y, the z position is kept positive to simulate the SERS substrate. While the surface dynamics are complex and can lead to distinctly non-Brownian diffusion[30] over time, we only simulate a single trapping event within the single hotspot. As soon as the particle exits the hotspot, the simulation stops and another one begins. While this will then miss re-entry of the same molecule into the hotspot, it still captures the behavior while the particle remains in the hotspot, which is the condition for SERS to occur. Since molecular random walks can lead to SERS fluctuations,[32] the intensity of the simulated SERS signal is simply mapped to the position of the particle in the hotspot.

With the above finite-difference scheme for simulating a Brownian particle in a potential well, we can vary the well depth and observe the time dynamics of the system. Figure 5 shows the simulation results. In Figure 5a, the particle begins at the origin, i.e. the center of the hotspot, and is allowed to diffuse using eq 3. For a trap depth on the order of the thermal energy k_BT, the particle easily escapes the trap. For a deeper trap on the order of 10 k_BT, the particle can remain trapped much longer. These numerical results agree with analytical models for the expected lifetime of a nanoparticle in a plasmonic trap,[33] where the ratio of trap depth to thermal energy should be ∼10 or more for stable trapping. Indeed, the expected time τ for a particle freely diffusing in three dimensions (without any optical forces) to travel a distance equal to the size of the hotspot δ will take the form $\tau = \frac{\delta^2}{6D}$. In our case, this is on the order of 10^{-7} s. The presence of the optical forces clearly lengthens this time, as shown by the simulated intensity trajectories in Figure 5b for the two trap depths. However, while the particle remains trapped, the signal still fluctuates as the particle randomly moves about within the volume of the trap. Figure 5c shows separate trajectories for a trapped particle at three different trap depths as well as a depiction of the coefficient of variation for these simulated signals. The deeper traps more tightly confine the particle near the trap's center, meaning that the coefficient of variation will be smaller. This is shown in Figure 5d for 1000 simulations, each with 50,000 time steps, at three different trap depths. The coefficient of variation histograms look qualitatively similar to the experimental histograms shown in Figure 4c. Comparing these coefficient of variation histograms suggests that a more tightly bound particle in a plasmonic hotspot, e.g. the "dry" and covalently bonded DTNB molecules, will on average generate individual SIF events with less internal fluctuations; a more loosely bound particle, e.g., the R6G molecules in liquid on the "wet" samples, will on average generate individual SIF events with more internal fluctuations. This is seen both experimentally and in the simulation results.

These results suggest that the timing statistics of multiple SIF events over a longer time span, e.g. the bursts and delays shown in Figures 1 and 2 for dry and wet environments, is perhaps more due to individual hotspot dynamics, rather than the molecular dynamics. In other words, to generate a SIF event, there needs to be both an available hotspot and an available molecule, and both have their own timing statistics. Comparing across all types of samples (DTNB dried, R6G dried, R6G wet) shows that the timing dynamics of the nanoparticle + molecule system have many similarities, regardless of the particular molecule, the local environment, or whether it may have a fluorescence signal background. While efficient SERS substrates tend to increase the SERS-to-fluorescence ratio,[34] our experiments with both fluorescent (R6G) and nonfluorescent (DTNB) molecules show many similarities in the overall timing statistics of the signal fluctuations. In particular, the most probable instantaneous SIF rate is in the several kHz range along with ∼0.01 s to ∼1 s delays across all samples and molecules; the most probable SIF

https://doi.org/10.1021/acs.jpcc.2c00319
J. Phys. Chem. C 2022, 126, 7117−7126

duration is in the several 100 μs range, with the dry samples having slightly longer events. While several factors may artificially increase (more hotspots under the laser spot) or decrease (fewer hotspots under the laser spot) the instantaneous SIF rates as discussed in Figure 3, these results suggest that perhaps the optical dynamics of the Ag nanoparticles themselves dominate the SIF behavior over the ∼10 μs to ∼1 s time scales. The highest-speed dynamics, on the order of <10 μs that are represented by the coefficient of variation, seem to therefore be due to particular molecule-in-hotspot effects; the high-speed SIF dynamics on the order of 10 μs to 1 s seem to be due more to silver adatom/hotspot rearrangements. While the dry samples of R6G and DTNB both had on average slightly longer SIF durations, perhaps due to a surface-stabilizing effect of the molecular coating, the coefficient of variation within a single SIF event revealed the largest differences between the wet and dry environments.

CONCLUSION

We explored high-speed SERS fluctuations in both dry and aqueous environments. The signal statistics could be categorized by several time-scale and intensity fluctuation effects. In particular, the wet environment showed extremely high-speed fluctuations during a single SIF event, whereas a dried and more stable molecule-hotspot environment showed SIF events with less variation. Both environments still displayed strong overall SIF behavior, with the dry particles on average having slightly longer events. These results provide some new insight into the underlying mechanisms of high-speed SERS fluctuations and may prompt further studies and applications of SERS in a variety of environments and for various metal−molecule systems.

ASSOCIATED CONTENT

Supporting Information

The Supporting Information is available free of charge at https://pubs.acs.org/doi/10.1021/acs.jpcc.2c00319.

Additional experimental data with more samples and analysis of the SIF detection algorithm. (PDF)

AUTHOR INFORMATION

Corresponding Authors

Nathan C. Lindquist − *Department of Physics and Engineering, Bethel University, St Paul, Minnesota 55112, United States;* orcid.org/0000-0002-1226-5212; Email: n-lindquist@bethel.edu

Alexandre G. Brolo − *Department of Chemistry, University of Victoria, Victoria, BC V8P 5C2, Canada; Centre for Advanced Materials and Related Technologies (CAMTEC), University of Victoria, Victoria, BC V8W 2Y2, Canada;* orcid.org/0000-0002-3162-0881; Email: agbrolo@uvic.ca

Author

Ariadne Tückmantel Bido − *Department of Chemistry, University of Victoria, Victoria, BC V8P 5C2, Canada; Centre for Advanced Materials and Related Technologies (CAMTEC), University of Victoria, Victoria, BC V8W 2Y2, Canada*

Complete contact information is available at: https://pubs.acs.org/10.1021/acs.jpcc.2c00319

Notes

The authors declare no competing financial interest.

ACKNOWLEDGMENTS

N.C.L. acknowledges support from the National Science Foundation (NSF), Awards 1552642 and 2003750. A.G.B. acknowledges operational grant support from the Natural Sciences and Engineering Research Council of Canada (NSERC), and instrument grant support from the Canada Foundation for Innovation (CFI), the British Columbia Knowledge Development Fund (BCKDF), and the University of Victoria.

REFERENCES

(1) Langer, J.; Jimenez de Aberasturi, D.; Aizpurua, J.; Alvarez-Puebla, R. A.; Auguié, B.; Baumberg, J. J.; Bazan, G. C.; Bell, S. E.; Boisen, A.; Brolo, A. G.; Choo, J.; Cialla-May, D.; Deckert, V.; Fabris, L.; Faulds, K.; García de Abajo, F. J.; Goodacre, R.; Graham, D.; Haes, A. J.; Haynes, C. L.; et al. Present and future of surface-enhanced Raman scattering. *ACS Nano* **2020**, *14*, 28−117.

(2) Fan, M.; Andrade, G. F.; Brolo, A. G. A review on the fabrication of substrates for surface enhanced Raman spectroscopy and their applications in analytical chemistry. *Anal. Chim. Acta* **2011**, *693*, 7−25.

(3) Fan, M.; Andrade, G. F.; Brolo, A. G. A review on recent advances in the applications of surface-enhanced Raman scattering in analytical chemistry. *Anal. Chim. Acta* **2020**, *1097*, 1−29.

(4) Pérez-Jiménez, A. I.; Lyu, D.; Lu, Z.; Liu, G.; Ren, B. Surface-enhanced Raman spectroscopy: benefits, trade-offs and future developments. *Chemical Science* **2020**, *11*, 4563−4577.

(5) Ding, S.-Y.; You, E.-M.; Tian, Z.-Q.; Moskovits, M. Electromagnetic theories of surface-enhanced Raman spectroscopy. *Chem. Soc. Rev.* **2017**, *46*, 4042−4076.

(6) Shin, H.-H.; Yeon, G. J.; Choi, H.-K.; Park, S.-M.; Lee, K. S.; Kim, Z. H. Frequency-domain proof of the existence of atomic-scale SERS hot-spots. *Nano Lett.* **2018**, *18*, 262−271.

(7) Benz, F.; Schmidt, M. K.; Dreismann, A.; Chikkaraddy, R.; Zhang, Y.; Demetriadou, A.; Carnegie, C.; Ohadi, H.; De Nijs, B.; Esteban, R.; Aizpurua, J.; Baumberg, J. J. Single-molecule optomechanics in "picocavities". *Science* **2016**, *354*, 726−729.

(8) Nie, S.; Emory, S. R. Probing single molecules and single nanoparticles by surface-enhanced Raman scattering. *Science* **1997**, *275*, 1102−1106.

(9) Chikkaraddy, R.; De Nijs, B.; Benz, F.; Barrow, S. J.; Scherman, O. A.; Rosta, E.; Demetriadou, A.; Fox, P.; Hess, O.; Baumberg, J. J. Single-molecule strong coupling at room temperature in plasmonic nanocavities. *Nature* **2016**, *535*, 127−130.

(10) Wrzosek, B.; Kitahama, Y.; Ozaki, Y. SERS Blinking on Anisotropic Nanoparticles. *J. Phys. Chem. C* **2020**, *124*, 20328−20339.

(11) Yamamoto, Y. S.; Ishikawa, M.; Ozaki, Y.; Itoh, T. Fundamental studies on enhancement and blinking mechanism of surface-enhanced Raman scattering (SERS) and basic applications of SERS biological sensing. *Frontiers of Physics* **2014**, *9*, 31−46.

(12) dos Santos, D. P.; Temperini, M. L.; Brolo, A. G. Intensity Fluctuations in Single-Molecule Surface-Enhanced Raman Scattering. *Acc. Chem. Res.* **2019**, *52*, 456−464.

(13) Lindquist, N. C.; Brolo, A. G. Ultra-High-Speed Dynamics in Surface-Enhanced Raman Scattering. *J. Phys. Chem. C* **2021**, *125*, 7523−7532.

(14) Lindquist, N. C.; de Albuquerque, C. D. L.; Sobral-Filho, R. G.; Paci, I.; Brolo, A. G. High-speed imaging of surface-enhanced Raman scattering fluctuations from individual nanoparticles. *Nat. Nanotechnol.* **2019**, *14*, 981−987.

(15) de Albuquerque, C. D. L.; Hokanson, K. M.; Thorud, S. R.; Sobral-Filho, R. G.; Lindquist, N. C.; Brolo, A. G. Dynamic imaging of multiple SERS hotspots on single nanoparticles. *ACS Photonics* **2020**, *7*, 434−443.

(16) Bido, A. T.; Nordberg, B. G.; Engevik, M. A.; Lindquist, N. C.; Brolo, A. G. High-Speed Fluctuations in Surface-Enhanced Raman Scattering Intensities from Various Nanostructures. *Appl. Spectrosc.* **2020**, *74*, 1398−1406.
(17) Emory, S. R.; Jensen, R. A.; Wenda, T.; Han, M.; Nie, S. Re-examining the origins of spectral blinking in single-molecule and single-nanoparticle SERS. *Faraday Discuss.* **2006**, *132*, 249−259.
(18) Miller, H.; Zhou, Z.; Shepherd, J.; Wollman, A. J.; Leake, M. C. Single-molecule techniques in biophysics: a review of the progress in methods and applications. *Rep. Prog. Phys.* **2018**, *81*, 024601.
(19) Margueritat, J.; Bouhelier, A.; Markey, L.; Colas des Francs, G.; Dereux, A.; Lau-Truong, S.; Grand, J.; Lévi, G.; Félidj, N.; Aubard, J.; Finot, E. Discerning the origins of the amplitude fluctuations in Dynamic Raman nanospectroscopy. *J. Phys. Chem. C* **2012**, *116*, 26919−26923.
(20) Itoh, T.; Yamamoto, Y. S. Recent topics on single-molecule fluctuation analysis using blinking in surface-enhanced resonance Raman scattering: clarification by the electromagnetic mechanism. *Analyst* **2016**, *141*, 5000−5009.
(21) Lombardi, J. R.; Birke, R. L. A unified view of surface-enhanced Raman scattering. *Accounts of chemical research* **2009**, *42*, 734−742.
(22) Leopold, N.; Lendl, B. A new method for fast preparation of highly surface-enhanced Raman scattering (SERS) active silver colloids at room temperature by reduction of silver nitrate with hydroxylamine hydrochloride. *J. Phys. Chem. B* **2003**, *107*, 5723−5727.
(23) Huff, J. The Airyscan detector from ZEISS: confocal imaging with improved signal-to-noise ratio and super-resolution. *Nat. Methods* **2015**, *12*, i.
(24) Lee, J.; Crampton, K. T.; Tallarida, N.; Apkarian, V. A. Visualizing vibrational normal modes of a single molecule with atomically confined light. *Nature* **2019**, *568*, 78.
(25) Willets, K. A.; Wilson, A. J.; Sundaresan, V.; Joshi, P. B. Super-resolution imaging and plasmonics. *Chem. Rev.* **2017**, *117*, 7538−7582.
(26) Stranahan, S. M.; Willets, K. A. Super-resolution optical imaging of single-molecule SERS hot spots. *Nano Lett.* **2010**, *10*, 3777−3784.
(27) Olson, A. P.; Spies, K. B.; Browning, A. C.; Soneral, P. A.; Lindquist, N. C. Chemically imaging bacteria with super-resolution SERS on ultra-thin silver substrates. *Sci. Rep.* **2017**, *7*, 9135.
(28) Wertz, E.; Isaacoff, B. P.; Flynn, J. D.; Biteen, J. S. Single-molecule super-resolution microscopy reveals how light couples to a plasmonic nanoantenna on the nanometer scale. *Nano Lett.* **2015**, *15*, 2662−2670.
(29) Devore, J. L. *Probability and Statistics for Engineering and the Sciences*, 8th ed.; Julet, M., Ed.; Cengage Learning: 2011; p 44.
(30) Wang, D.; Schwartz, D. K. Non-Brownian Interfacial Diffusion: Flying, Hopping, and Crawling. *J. Phys. Chem. C* **2020**, *124*, 19880−19891.
(31) Volpe, G. Simulation of a Brownian particle in an optical trap. *American Journal of Physics* **2013**, *81*, 224−230.
(32) Kitahama, Y.; Araki, D.; Yamamoto, Y. S.; Itoh, T.; Ozaki, Y. Different behaviour of molecules in dark SERS state on colloidal Ag nanoparticles estimated by truncated power law analysis of blinking SERS. *Phys. Chem. Chem. Phys.* **2015**, *17*, 21204−21210.
(33) Davis, T. Brownian diffusion of nano-particles in optical traps. *Opt. Express* **2007**, *15*, 2702−2712.
(34) Sadegh, N.; Khadem, H.; Tavassoli, S. H. High Raman-to-fluorescence ratio of Rhodamine 6G excited with 532 nm laser wavelength using a closely packed, self-assembled monolayer of silver nanoparticles. *Appl. Opt.* **2016**, *55*, 6125−6129.

https://doi.org/10.1021/acs.jpcc.2c00319
J. Phys. Chem. C 2022, 126, 7117−7126